IOSR Journal Of Applied Physics (IOSR-JAP)
e-ISSN: 2278-4861.Volume 16, Issue 5 Ser. 1 (Sept. – Oct. 2024), PP 42-49
www.Iosrjournals.Org

Spectral, Thermal and Upconversion Properties of Dy^{3+} Doped Borotellurite Glasses with Large Stability Parameter

S.L.Meena
Ceramic Laboratory, Department of physics, Jai Narain Vyas University, Jodhpur 342001(Raj.) India
E-mail address:shankardiya7@rediffmail.com

Abstract
Glass sample of yttrium zinc lithium lead sodium alumino borotellurite (25-x) TeO_2:10ZnO:10Li_2O:10PbO:10Na_2O:10Al_2O_3:10Y_2O_3:15B_2O_3:xDy_2O_3. (wherex=1,1.5 and 2 mol%) have been prepared by melt-quenching technique. The amorphous nature of the prepared glass samples was confirmed by X-ray diffraction. Optical absorption, excitation spectrum and fluorescence spectra were recorded at room temperature for all glass samples. Judd-Ofelt intensity parameters Ω_λ (λ=2, 4 and 6) are evaluated from the intensities of various absorption bands of optical absorption spectra. Using these intensity parameters various radiative properties like spontaneous emission probability, branching ratio, radiative life time and stimulated emission cross–section of various emission lines have been evaluated

Keywords: *YZLLSABT Glasses, Thermal Analysis, Optical Properties, Judd-Ofelt Theory, Thermal properties.*

Date of Submission: 27-09-2024 Date of Acceptance: 09-10-2024

I. Introduction

Glasses doped with trivalent rare earth doped are very important due to its potential applications in areas such as optical data storage, optoelectronic device, solid state lasers, optical fibers for communication, photoelectronic device and optical amplifier media [1-5]. Among different glasses, tellurite glasses have unique properties. They have high transparency, high refractive index, high density and high thermal stability. Borotellurite glasses possess interesting properties like lower phonon energy, high gain density, high solubility, low melting temperature and non-linear optical susceptibilities [6-11].Addition of network modifier (NWF) Li_2O to the borotellurite glasses improves both electrical and mechanical properties of such glasses [12, 13]. ZnO is also added due to its specific chemical and physical properties and boric acid acts as a good glass former and flux material. B_2O_3 glass network could significantly improve different properties like mechanical strength, thermal stability and chemical durability [14,15]. Al_2O_3 is often added to modify the glass structure that improves the physical properties, chemical durability and mechanical strength [16].The low glass melting temperature, high thermal stability, good rare earth ion solubility and the optical fiber development compatibility makes the borotellurite glasses suitable candidates for photonic applications[17,18]. Recently Dy^{3+} ions doped glasses found important in the area of wave guide laser, laser action and Telecommunications optical fibers [19-25].

The present work reports on the preparation and characterization of rare earth doped heavy metal oxide (HMO) glass systems for lasing materials. I have studied on the absorption and emission properties of Dy^{3+} doped yttrium zinc lithium lead sodium alumino borotellurite glasses. The intensities of the transitions for the rare earth ions have been estimated successfully using the Judd-Ofelt theory, The laser parameters such as radiative probabilities(A),branching ratio (β), radiative life time(τ_R) and stimulated emission cross section(σ_p) are evaluated using J.O.intensity parameters(Ω_λ, λ=2,4 and 6).

II. Experimental Techniques

Preparation of glasses

The following Dy^{3+}doped borotellurite glass samples (25-x) TeO_2:10ZnO:10Li_2O:10PbO:10Na_2O:10Al_2O_3:10Y_2O_3:15B_2O_3 xDy_2O_3. (where x=1,1.5 and 2 mol%) have been prepared by melt-quenching method. Analytical reagent grade chemical used in the present study consist of TeO_2, ZnO, Li_2O, PbO, Na_2O, Al_2O_3, Y_2O_3 ,B_2O_3 and Dy_2O_3. They were thoroughly mixed by using an agate pestle mortar. then melted at 1050^0C by an electrical muffle furnace for 2h., After complete melting, the melts were quickly poured in to a preheated stainless steel mould and annealed at temperature of 350^0C for 2h to remove thermal strains and stresses. Every time fine powder of cerium oxide was used for polishing the

samples. The glass samples so prepared were of good optical quality and were transparent. The chemical compositions of the glasses with the name of samples are summarized in **Table 1.**

Table 1.

Chemical composition of the glasses

Sample	Glass composition (mol %)
YZLLSABT (UD)	(25-x) TeO_2:10ZnO:10Li_2O:10PbO:10Na_2O:10Al_2O_3:10Y_2O_3:15B_2O_3
YZLLSABT (DY1)	34Bi_2O_3:10PbO:10Li_2O:10CdO:10Ta_2O_5:10MgO:15B_2O_3.1 Dy_2O_3.
YZLLSABT (DY1.5)	33.5Bi_2O_3:10PbO:10Li_2O:10CdO:10Ta_2O_5:10MgO:15B_2O_3.1.5 Dy_2O_3.
YZLLSABT (DY2)	33Bi_2O_3:10PbO:10Li_2O:10CdO:10Ta_2O_5:10MgO:15B_2O_3. 2 Dy_2O_3.

YZLLSABT (UD) -Represents undoped Yttrium Zinc Lithium Lead Sodium Alumino Borotellurite glass specimens.
YZLLSABT (DY)-Represents Dy^{3+} doped Yttrium Zinc Lithium Lead Sodium Alumino Borotellurite glass specimens.

III.Theory

3.1 Oscillator Strength

The intensity of spectral lines are expressed in terms of oscillator strengths using the relation [26].

$$f_{expt.} = 4.318 \times 10^{-9} \int \varepsilon(\nu)\, d\nu \qquad (1)$$

where, $\varepsilon(\nu)$ is molar absorption coefficient at a given energy ν (cm^{-1}), to be evaluated from Beer–Lambert law. Under Gaussian Approximation, using Beer–Lambert law, the observed oscillator strengths of the absorption bands have been experimentally calculated [27], using the modified relation:

$$P_m = 4.6 \times 10^{-9} \times \frac{1}{cl} \log \frac{I_0}{I} \times \Delta\upsilon_{1/2} \qquad (2)$$

where c is the molar concentration of the absorbing ion per unit volume, I is the optical path length, $\log I_0/I$ is optical density and $\Delta\upsilon_{1/2}$ is half band width.

3.2. Judd-Ofelt Intensity Parameters

According to Judd [28] and Ofelt [29] theory, independently derived expression for the oscillator strength of the induced forced electric dipole transitions between an initial J manifold $|4f^N (S, L) J\rangle$ level and the terminal J' manifold $|4f^N (S', L') J'\rangle$ is given by:

$$\frac{8\Pi^2 mc\bar{\upsilon}}{3h(2J+1)} \frac{1}{n}\left[\frac{(n^2+2)^2}{9}\right] \times S(J, J') \qquad (3)$$

Where, the line strength S (J, J') is given by the equation

$$S(J, J') = e^2 \sum_{\lambda=2,4,6} \Omega_\lambda \langle 4f^N(S, L) J \| U^{(\lambda)} \| 4f^N (S', L') J' \rangle^2 \qquad (4)$$

In the above equation m is the mass of an electron, c is the velocity of light, ν is the wave number of the transition, h is Planck's constant, n is the refractive index, J and J' are the total angular momentum of the initial and final level respectively, Ω_λ (λ=2,4and 6) are known as Judd-Ofelt intensity parameters.

3.3 Radiative Properties

The Ω_λ parameters obtained using the absorption spectral results have been used to predict radiative properties such as spontaneous emission probability (A) and radiative life time (τ_R), and laser parameters like fluorescence branching ratio (β_R) and stimulated emission cross section (σ_p).

The spontaneous emission probability from initial manifold $|4f^N (S', L') J'\rangle$ to a final manifold $|4f^N (S, L) J\rangle$ is given by:

$$A[(S', L') J'; (S, L) J] = \frac{64\pi^2\nu^3}{3h(2J'+1)}\left[\frac{n(n^2+2)^2}{9}\right] \times S(J', \bar{J}) \qquad (5)$$

Where, $S(J', J) = e^2 [\Omega_2 \| U^{(2)} \|^2 + \Omega_4 \| U^{(4)} \|^2 + \Omega_6 \| U^{(6)} \|^2]$

The fluorescence branching ratio for the transitions originating from a specific initial manifold $|4f^N (S', L') J'>$ to a final many fold $|4f^N (S, L) J >$ is given by

$$\beta [(S', L') J'; (S, L) J] = \frac{A[(S' L') J' (\bar{S} \bar{L})]}{\sum_{S L J} A[(S' L') J' (\bar{S} \bar{L})]} \quad (6)$$

where, the sum is over all terminal manifolds.

The radiative life time is given by

$$\tau_{rad} = \sum_{S L J} A[(S', L') J'; (S, L)] = A^{-1}_{Total} \quad (7)$$

where, the sum is over all possible terminal manifolds. The stimulated emission cross -section for a transition from an initial manifold $|4f^N (S', L') J'>$ to a final manifold $|4f^N (S, L) J >|$ is expressed as

$$\sigma_p(\lambda_p) = \left[\frac{\lambda_p^4}{8\pi c n^2 \Delta\lambda_{eff}}\right] \times A[(S', L') J'; (\bar{S}, \bar{L}) \bar{J}] \quad (8)$$

where, λ_p the peak fluorescence wavelength of the emission band and $\Delta\lambda_{eff}$ is the effective fluorescence line width.

IV. Result and Discussion

4.1 XRD Measurement

Figure 1 presents the XRD pattern of the sample contain – TeO_2 which is show no sharp Bragg's peak, but only a broad diffuse hump around low angle region. This is the clear indication of amorphous nature within the resolution limit of XRD instrument

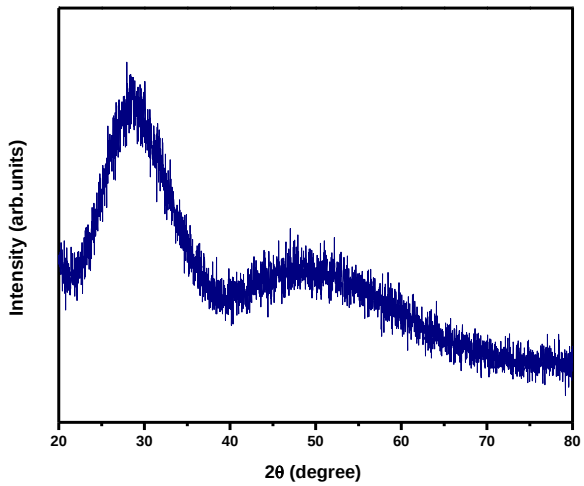

Fig. (1) X-ray diffraction pattern of YZLLSABT DY (01) glass.

4.2 Thermal Property

Differential thermal analysis checks the heat absorbed by glass samples during heating or cooling. Fig. 2 depicts the DTA thermogram of powdered YZLLSABT sample. The glass transition temperature (T_g), onset crystallization temperature (T_c), crystallization temperature (T_p), melting temperature(T_m), thermal stability (T_s), thermal stability parameter(S),Hurbe's criterion (H_r) and reduced glass transition temperature(T_{rg}) were calculated. All the determined thermal parameters are given in table 2.

Glass samples	T_g(℃)	T_c(℃)	T_p(℃)	T_m(℃)	T_s(℃)	H_r(℃)	S(℃)	T_{rg}(℃)
YZLLSABT DY(01)	376	507	546	685	131	0.219	13.59	0.549
YZLLSABT DY(1.0)	379	509	548	688	130	0.218	13.38	0.551
YZLLSABT DY(02)	381	510	553	692	129	0.236	14.56	0.551

The thermal stability of the glass samples can be calculated by difference between onset crystallization temperature and transition temperature [30].

Thermal stability (T_s) $=T_c-T_g$ (9)

Hruby's criterion is calculated using the Hurby's relation [31].

Hruby's criterion (H_r) $= [(T_p-T_c)/(T_m-T_c)$ (10)

Reduced glass transition temperature is given as [32].

Reduced glass transition temperature (T_{rg}) $=T_g/T_m$ (11)

Thermal stability parameter can be calculated using [33].

Thermal stability parameter (S) $= [(T_p-T_c) \times (T_c-T_g)]/ T_g$ (12)

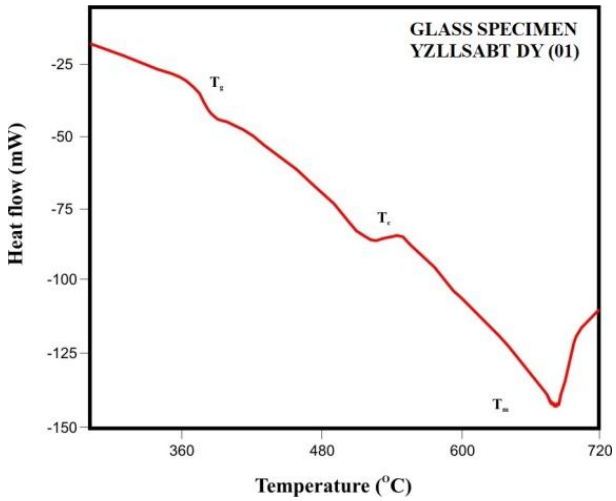

Fig.2: DTA curve of YZLLSABT DY (01) glass.

4.2 Absorption Spectrum

The absorption spectra of Dy^{3+}doped YZLLSABT glass specimens have been presented in Figure 2 in terms of Intensity versus wavelength. Thirteen absorption bands have been observed from the ground state $^6H_{15/2}$ to excited states $^6H_{13/2}$, $^6H_{11/2}$, $^6H_{9/2}+^6F_{11/2}$,$^6H_{7/2}+^6F_{9/2}$,$^6F_{7/2}+^6H_{5/2}$,$^6F_{5/2}$,$^6F_{3/2}$,$^6F_{9/2}$,$^4I_{15/2}$,$^4G_{11/2}$, $^6F_{7/2}+^4I_{13/2}$, $^6M_{19/2}+4(P,D)_{3/2}$ and $^4G_{9/2}+^6P_{3/2}$ for Dy^{3+}doped YZLLSABT glasses.

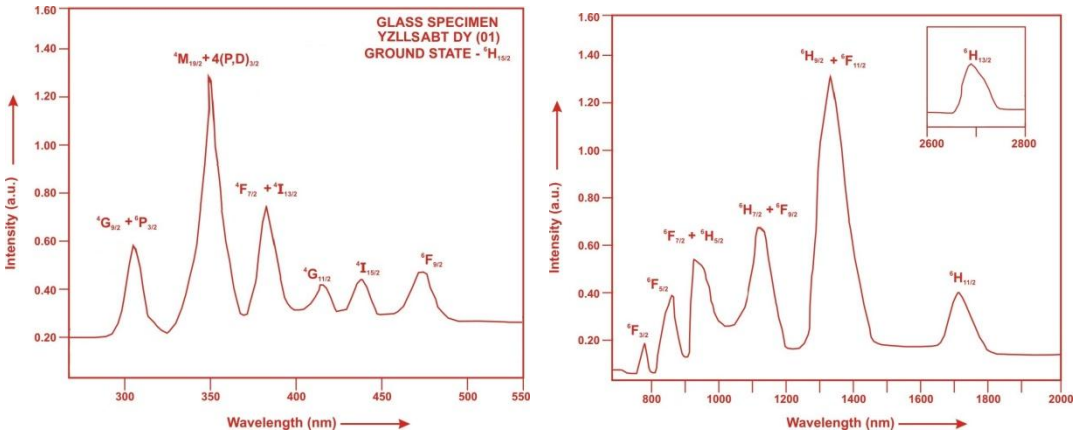

Fig. (3) Absorption spectrum of YZLLSABT DY (01) glass.

The experimental and calculated oscillator strength for Dy^{3+} ions in YZLLSABT glasses are given in **Table 2.**

Table 2: Measured and calculated oscillator strength ($P_m \times 10^{+6}$) of Dy^{3+}ions in YZLLSABT glasses.

Energy level from $^6H_{15/2}$	**Glass YZLLSABT (DY01)**		**Glass YZLLSABT (DY1.5)**		**Glass YZLLSABT (DY02)**	
	$P_{exp.}$	$P_{cal.}$	$P_{exp.}$	$P_{cal.}$	$P_{exp.}$	$P_{cal.}$
$^6H_{13/2}$	2.14	2.43	2.12	2.42	2.09	2.40
$^6H_{11/2}$	1.52	2.07	1.49	2.05	1.45	2.02
$^6H_{9/2}$+$^6F_{11/2}$	10.35	10.25	10.30	10.20	10.28	10.18
$^6H_{7/2}$+$^6F_{9/2}$	5.62	5.31	5.58	5.28	5.55	5.25
$^6F_{7/2}$+$^6H_{5/2}$	4.78	3.85	4.75	3.81	4.72	3.76
$^6F_{5/2}$	1.38	1.75	1.35	1.73	1.33	1.70
$^6F_{3/2}$	0.37	0.33	0.35	0.33	0.33	0.32
$^6F_{9/2}$	0.41	0.29	0.39	0.29	0.36	0.29
$^4I_{15/2}$	0.35	0.72	0.32	0.71	0.30	0.70
$^4G_{11/2}$	0.29	0.17	0.26	0.17	0.24	0.17
$^6F_{7/2}$+$^4I_{13/2}$	3.57	3.74	3.54	3.71	3.51	3.68
$^6M_{19/2}$+4(P,D)3/2	7.98	9.98	7.95	9.97	7.93	9.97
$^4G_{9/2}$+$^6P_{3/2}$	1.72	2.12	1.69	2.11	1.66	2.08
r.m.s. deviation	0.6719		0.6772		0.6857	

*Low r.m.s. deviation values clearly indicate the accuracy of fitting.

The values of Judd-Ofelt intensity parameters are given in **Table 3.**

Table 3: Judd-Ofelt intensity parameters for Dy^{3+} doped YZLLSABT glass specimens

Glass Specimen	**Ω_2(pm^2)**	**Ω_4(pm^2)**	**Ω_6(pm^2)**	**Ω_4 /Ω_6**	**Trend**	**Ref.**
YZLLSABT (DY01)	2.889	1.658	1.466	1.131	**$\Omega_2 > \Omega_4 > \Omega_6$**	P.W.
YZLLSABT (DY1.5)	2.868	1.661	1.447	1.148	**$\Omega_2 > \Omega_4 > \Omega_6$**	P.W.
YZLLSABT (DY02)	2.853	1.674	1.420	1.179	**$\Omega_2 > \Omega_4 > \Omega_6$**	P.W.
ATFP (DY)	5.53	2.13	0.88	2.420	**$\Omega_2 > \Omega_4 > \Omega_6$**	[34]
PHTA (DY)	10.17	4.32	3.27	1.321	**$\Omega_2 > \Omega_4 > \Omega_6$**	[35]
BFB (DY)	2.90	1.09	0.98	1.112	**$\Omega_2 > \Omega_4 > \Omega_6$**	[36]

4.3 Excitation Spectrum

The Excitation spectra of Dy^{3+}doped YZLLSABT glass specimens have been presented in Figure 4 in terms of Excitation Intensity versus wavelength. The excitation spectrum was recorded in the spectral region 315–480 nm fluorescence at 575nm having different excitation band centered at 322,353, 365, 385, 425, 454 and 473 nm are attributed to the $^6P_{3/2}$, $^6P_{7/2}$, $^4P_{3/2}$, $^4I_{13/2}$, $^4G_{11/2}$, $^4I_{15/2}$ and $^4F_{9/2}$ transitions, respectively. The highest absorption level is $^4I_{13/2}$ and is at 385nm.So this is to be chosen for excitation wavelength.

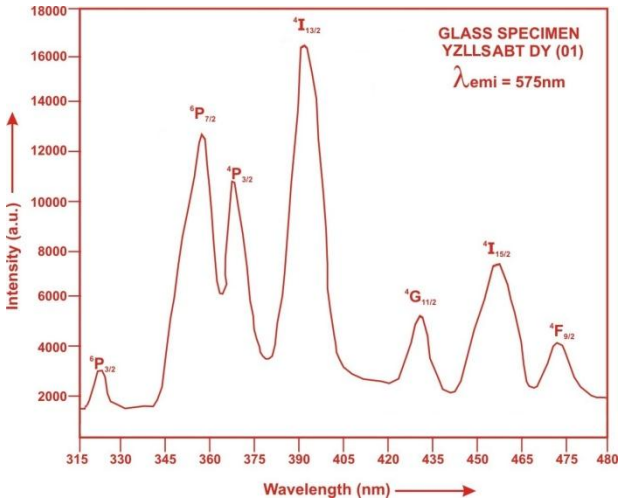

Fig. (4) Excitation spectrum of YZLLSABT DY (01) glass.

4.4. Fluorescence Spectrum

The fluorescence spectrum of Dy^{3+}doped in yttrium zinc lithium lead sodium alumino borotellurite glass is shown in Figure 5. There are three broad bands observed in the Fluorescence spectrum of Dy^{3+}doped yttrium zinc lithium lead sodium alumino borotellurite glass. The wavelengths of these bands along with their assignments are given in Table 6. The peak with maximum emission intensity appears at 485nm, 575 nm 665 nm and 752 nm and corresponds to the ($^4F_{9/2}\rightarrow{}^6H_{15/2}$), ($^4F_{9/2}\rightarrow{}^6H_{13/2}$) and ($^4F_{9/2}\rightarrow{}^6H_{11/2}$) transition.

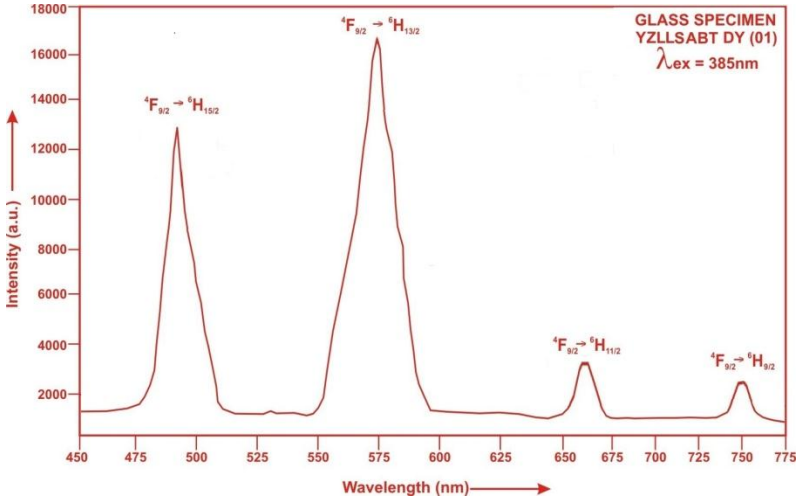

Fig. (5). Fluorescence spectrum of YZLLSABT DY (01) glass.

Table4: Emission peak wave lengths (λ_p),radiative transition probability (A_{rad}),branching ratio (β),stimulated emission cross-section(σ_p) and radiative life time(τ_R) for various transitions in Dy^{3+} doped YZLLSABT glasses.

Transition		YZLLSABT DY 01				YZLLSABT DY 1.5				YZLLSABT DY 02			
	λ_{max} (nm)	$A_{rad}(s^{-1})$	β	σ_p (10^{-20} cm^2)	τ_R(μs)	$A_{rad}(s^{-1})$	β	σ_p (10^{-20} cm^2)	τ_R (μs)	$A_{rad}(s^{-1})$	β	σ_p (10^{-20} cm^2)	τ_R (10^{-20} cm^2)
$^4F_{9/2}\rightarrow{}^6H_{15/2}$	485	83.52	0.1994	0.165	2386.77	82.79	0.1990	0.161	2403.17	81.75	0.1979	0.155	2420.27
$^4F_{9/2}\rightarrow{}^6H_{13/2}$	575	282.42	0.6741	1.199		280.54	0.6742	1.171		278.83	0.6748	1.136	
$^4F_{9/2}\rightarrow{}^6H_{11/2}$	665	29.72	0.0709	0.145		29.56	0.0710	0.142		29.44	0.0713	0.139	
$^4F_{9/2}\rightarrow{}^6H_{9/2}$	752	23.32	0.0557	0.138		23.22	0.0558	0.135		23.16	0.0560	0.133	

V. Conclusion

In the present study, the glass samples of composition (25-x) TeO_2:10ZnO:10 Li_2O:10 PbO: 10Na_2O:10Al_2O_3:10 Y_2O_3:15B_2O_3:xDy_2O_3 (where x =1, 1.5and 2mol %) have been prepared by melt-quenching method. The thermal stability parameter for prepared glass samples are very large.The value of stimulated emission cross-section (σ_p) is found to be maximum for the transition ($^4F_{9/2}\rightarrow{}^6H_{13/2}$) for all glass specimens. This shows that ($^4F_{9/2}\rightarrow{}^6H_{13/2}$) transition is most probable transition.

References

[1]. H.M.Zakaly,A.S.Abouhaswa,S.A.M.Issa,M.Y.A.Mostafa,M.Pyshkina,Optical and nuclear radiation shielding properties of zinc borate glasses doped with lanthanum oxide,J.Lumin.543,120151(2020).

[2]. S.L.Meena, Structural,physical and optical properties of Pr^{3+} doped in bismuth borate glasses,Appl. Phys. A,130:404,1-12(2024).

[3]. I. Kashif ,A. Ratep, S.Ahmed, Spectroscopic properties of lithium borate glass containing Sm^{3+} and Nd^{3+} ions, Int. J. of Adv. in App. Sci. 9(3), 211-219(2020).

[4]. A.S.Abouhaswa,Y.S.Rammah,S.E.Ibrahim,A.A.El-Hamalaway, Structural,optical and electrical characterization of borate glasses doped with SnO_2,J.Lumin.494,59-65(2018).

[5]. P.S.Wong,M.H.Hussin,Lintang,H.O.Lintang,S.Endud, Structural and luminescence studies of europium ions in lithium aluminium borophosphate glasses,J. Rare Earth 32,585-592(2014).

[6]. N.Boudchicha,M.Iezid,F.Goumeidane,M.Legouera,P.S.Prasad,P.V.Rao, Judd–Ofelt Analysis and Spectroscopy Study of Tellurite Glasses Doped with Rare-Earth (Nd^{3+}, Sm^{3+}, Dy^{3+}, and Er^{3+}),Materials,16,6832,1-19(2023).

[7]. F.Ren,Y.Z.Mei,C.Gao,L.G.Zhu,A.Lu, Thermal stability and Judd-Ofelt analysis of optical properties of Er^{3+} doped tellurite glasses, Trans. Nonferrous Met. Soc. China, 22, 2021–2026(2012).

[8]. H.Elkholy,H. Othman,I. Hager,M.Ibrahim,D. de Ligny, Thermal and optical properties of binary magnesium tellurite glasses and their link to the glass structure. J. Alloys Compd.823, 153781(2020).

[9]. R.A.A.Silva,N.F.Dantas,R.F.Muniz,R.F.Muniz,A.M.O.Lima,F.Pedrochi,A.Steimacher,M.J.Barboza, Optical and Spectroscopic properties of Er^{3+}/Yb^{3+} co-doped calcium borotellurite glasses,J.Lumin.251,119239(2022).

[10]. N.Elkhoshkhany,S. Marzouk,M. El-Sherbiny,H. Ibrahim,B. Burtan-Gwizdala,M.S. Alqahtani,K.I. Hussien, M. Reben,E.S. Yousef, Investigation of structural, physical, and attenuation parameters of glass: TeO_2 -Bi_2O_3 -B_2O_3 -TiO_2 -RE_2O_3 (RE: La, Ce, Sm, Er, and Yb), and applications thereof. Materials, 15, 5393(2022).

[11]. S.L.Meena,Spectral and Raman analysis of Er^{3+} doped zinc lithium antimony sodalime tellurite glasses,Int.J.Eng.Sci.Invent.10,09-15(2021).

[12]. J. Anjaiah, C. Laxmikanth, Optical Properties of Neodymium Ion Doped Lithium Borate Glasses, 5,173 -183(2015).

[13]. R. Devi, C. K.Jayasankar , Optical properties of Nd^{3+} ions in lithium borate glasses, Materials chemistry and physics, 42,106-119(1995).

[14]. M.Peng, L.Wondraczek , Bismuth-Doped Oxide Glasses as Potential Solar Spectral Converters and Concentrators, J. Mater. Chem., 19,627-630(2009).

[15]. D.L. Griscon, Materials Science Research, Borate Glasses, vol. 12 Plenum, New York, p. 36(1978).

[16]. H.A.Othman, G.M. Arzumanyan , D.Moncke, The influence of different alkaline earth oxide on the structural and optical properties of undoped, Ce-doped, Sm-doped and Sm/Ce coped lithium alumino-phosphate glasses,Optical Materials,62,689-696(2016).

[17]. S.L.Meena, Spectral and FTIR analysis of Ho^{3+} ions doped zinc lithium sodium potassium gallium borotellurite glasses, Int.J.Inn.Res.Sci.Eng.Tech.12,10835-10843(2023).

[18]. S.Stalin,D. Gaikwad,M. Samee,A. Edukondalu,S.K. Ahmmad,A. Joshi,R. Syed, Structural, optical features and gamma ray shielding properties of Bi_2O_3– TeO_2– B_2O_3 -GeO_2 glass system. Ceram. Int. 46, 17325–17334(2020).

[19]. Z.Hong,H.Yue,G. Gong,F.Lai,Z.Zou,W.You,S.Wu,J. Huang, Spectroscopic study of Dy^{3+} ions doped gallium silicate glasses for yellow solid state lasers, Silicon, 16,463-470(2024).

[20]. M.Babu,B.C.Jamalaiah,J.S.Kumar,T.Sasikala,L.R.Moorthy,Spectroscopic and Photoluminescence properties of Dy^{3+} doped lead tungsten tellurite glasses for laser materials,509(2),457-462(2011).

[21]. N.Jaidass,C.K.Moorthi,A.M.Babu, M.R.Babu, Luminescence properties of Dy^{3+} doped lithium zinc borosilicate glasses for photonic applications,Heliyon,4(3),e00555(2018).

[22]. W.A. Pisarski, Judd–Ofelt Analysis and Emission Properties of Dy^{3+} Ions in Borogermanate Glasses, Materials, 15, 9042(2022).

[23]. A.M. Babu, B.C. Jamalaiah, J.S. Kumar, T. Sasikala, L.R. Moorthy, Spectroscopic and photoluminescence properties of Dy^{3+} doped lead tungsten tellurite glasses for laser materials. J Alloys Compd. 509,457–462(2011).

[24]. S. Kumar P, K. Marimuthu, Investigation on spectroscopic properties of Dy^{3+} doped zinc telluro-fluoroborate glasses for laser and white LED applications. J Mol. Struct. 1125, 443–52(2016).

[25]. P.P.Pawar, S.R. Munishwar, R.S. Gedam, Physical and optical properties of Dy^{3+}/Pr^{3+} co-doped lithium borate glasses for W-LED. J Alloys Compd.660,347–55(2016).

[26]. C. Gorller-Walrand,K. Binnemans, Spectral Intensities of f-f Transition. In: Gshneidner Jr., K.A. and Eyring,L., Eds., Handbook on the Physics and Chemistry of Rare Earths, Vol. 25, Chap. 167, North-Holland, Amsterdam, 101-264(1988).

[27]. Y.K.Sharma, S.S.L.Surana,R.K.Singh, Spectroscopic Investigations and Luminescence Spectra of Sm^{3+} Doped Soda Lime Silicate Glasses. Journal of Rare Earths, 27, 773(2009).

[28]. B.R. Judd, Optical absorption intensities of rare earth ions,Phys.Rev.127,750-761(1962).

[29]. G.S.Ofelt, Intensities of crystal spectra of rare earth Ions, Chem.Phys37, 511-520(1962).

[30]. B.Karthikeyan, S.Mohan, Structural,Optical And Glass Transition Studies On Nd^{3+} Doped Lead Bismuth Borate Glasses,Phys.B.334,298-302(2003).

[31]. A.Hurby, Evaluation Of Glass –Forming Tendency By Means Of Dta.Czech.J.Phys.B.22,1187-1193(1972).

[32]. V.Kumar,S.Sharma,O.P.Pandey,K.Singh, Thermal And Physical Properties of $30SrO\text{-}40SiO_2\text{-}20B_2O_3\text{-}10A_2O_3$(A=La,Y,Al) Glasses And Their Chemical Reaction With Bismuth Vanadate For Sofc.Solid State Ionic,181,79-85(2010).

[33]. M.Shwetha,B.Eraiah, Influence Of Er^{3+} Ions On The Physical,Structural,Optical And Thermal Properties Of $ZnO\text{-}Li_2O\text{-}P_2O_5$ Glasses, Appl.Phys.221,1-11(2019).

[34]. M.Jayasimhadri,L.R.Moorthy,K.Kojima,K.Yamamoto,N.Wada(1),N.Wada(2).Optical properties of Dy^{3+} ions in alkali tellurofluorophosphate glasses for laser materials,J.Phys.D,Appl.Phys.39,635-641(2006).

[35]. B.C. Jamalaiah,L.Rama Moorty,H.J.Seo, Effect of lead oxide on optical properties of Dy^{3+} ions in $PbO\text{-}H_3BO_3\text{-}TiO_2\text{-}AlF_3$ glasses,J.Non-Cryst.Solids,358:204-9(2012).

[36]. Y.Dwivedi, S.B. Rai, Spectroscopic study of Dy^{3+} and Dy^{3+}/Yb^{3+} ions co-doped in barium fluoroborate glass,Opt.Mater,31:1472-7(2009).